Clim Dyn (2011) 37:2455–2469
DOI 10.1007/s00382-011-1027-z

A comparison of climatological subseasonal variations in the wintertime storm track activity between the North Pacific and Atlantic: local energetics and moisture effect

Sun-Seon Lee · June-Yi Lee · Bin Wang · Fei-Fei Jin · Woo-Jin Lee · Kyung-Ja Ha

Received: 6 June 2010 / Accepted: 7 February 2011 / Published online: 23 February 2011

Abstract Distinct differences of the storm track–jet relationship over the North Pacific and North Atlantic are investigated in terms of barotropic and baroclinic energetics using NCEP-2 reanalysis data for the period of 1979–2008. From fall to midwinter the Pacific storm track (PST) activity weakens following the southward shift of the Pacific jet, whereas the Atlantic storm track (AST) activity remains steady in position and intensifies regardless of the slight southward shift of the Atlantic jet. This study is devoted to seeking for the factors that can contribute to this conspicuous difference between the two storm tracks on climatological subseasonal variation by analyzing eddy properties and local energetics. Different eddy properties over the two oceans lead to different contribution of barotropic energy conversion to the initiation of storm tracks. In the North Atlantic, meridionally elongated eddies gain kinetic energy efficiently from stretching deformation of the mean flow in the jet entrance. On the other hand, the term associated with shearing deformation is important for the initiation of PST. Analysis of baroclinic energetics reveals that the intensification of the AST activity in midwinter is mainly attributed to coincidence between location of maximum poleward and upward eddy heat fluxes and that of the largest meridional temperature gradient over slight upstream of the AST. The relatively large amount of precipitable water and meridional eddy moisture flux along baroclinic energy conversion axis likely provides a more favorable environment for baroclinic eddy growth over the North Atlantic than over the North Pacific. In the meantime, the midwinter minimum of the PST activity is attributable to the southward shift of the Pacific jet stream that leads to discrepancy between core region of poleward and upward heat fluxes and that of meridional thermal gradient. Weakening of eddy-mean flow interaction due to eddy shape and reduction of moist effect are also responsible for the weakening of storm track activities in midwinter when the strongest baroclinicity exists over the North Pacific.

Keywords Pacific and Atlantic storm tracks · Eddy-mean flow interaction · Barotropic and baroclinic energy conversion · Moisture effect

S.-S. Lee · K.-J. Ha (✉)
Division of Earth Environmental System,
Pusan National University, Busan, Korea
e-mail: kjha@pusan.ac.kr

J.-Y. Lee · B. Wang · F.-F. Jin
School of Ocean and Earth Science and Technology,
University of Hawaii, Honolulu, HI, USA

W.-J. Lee
Korea Meteorological Administration, Seoul, Korea

1 Introduction

The storm track, as represented by the region of enhanced synoptic transient activities, is one of the most important atmospheric circulation systems, which influences the weather and climate over the midlatitude regions in the Northern Hemisphere (NH) (e.g. Chang et al. 2002; Greeves et al. 2007; Nie et al. 2008). Synoptic-scale transient eddies in the storm track regions develop baroclinically. The structural and dynamical property and variability of synoptic-scale transient eddies over the North Pacific is different from that over the North Atlantic (e.g. Nakamura 1992; Chang et al. 2002; Nakamura et al. 2002).

In subseasonal time scale, the activity of the two storm tracks shows distinct characteristics. Nakamura (1992)

found that the Pacific storm track (hereafter, 'PST') activity is characterized by distinctive double peaks in late fall and early spring with midwinter suppression in spite of the strongest baroclinicity, whereas the Atlantic storm track (hereafter, 'AST') activity shows a single maximum in midwinter. It was shown that baroclinic wave activity over the North Pacific is positively correlated with the speed of westerly jet up to $\sim$45 ms^{-1}. When the speed of Pacific jet exceeds 45 ms^{-1}, the intensity of PST activity decreases with increasing jet strength. He also suggested that excessively strong advection by the jet may lead to the midwinter suppression; meanwhile relatively high lower tropospheric specific humidity and "seeding" perturbation coming from Siberia may play a role on enhancing transient activity during spring and fall. Chang (2001) found that the diabatic heating due to latent heat release helps amplify the baroclinic wave more effectively in October than in January. Nakamura and Sampe (2002) suggested that excessively intensified subtropical jet acts to hinder the eddy amplification by its trapping effect.

From the energetics point of view, it was shown that significant enhancement of the barotropic damping relative to the baroclinic growth in midwinter over the North Pacific is a major contributing factor to midwinter suppression of the PST activity (Deng and Mak 2006). Nakamura et al. (2002) showed that the stronger correlation between eddy temperature and eddy meridional (or vertical) velocity in the presence of the weakened westerlies indicates more efficient baroclinic energy conversion (BCEC), implying the optimum structure of transient eddies for baroclinic growth.

Barotropic and baroclinic dynamics play an important role on the storm track activity. Frisius et al. (1998) analyzed the physical mechanisms for the storm track organization in terms of the local energetics and transient eddy diagnostics. Based on the local energetics, they showed that local baroclinic instability is responsible for the enhanced eddy kinetic energy (EKE) in the downstream of the jet. Using reanalysis data and simulations of the General Circulation Model, Black and Dole (2000) examined the relationship between the barotropic deformation field and winter storm track activity and revealed that the horizontal structure of storm track activity in the climate model is strongly influenced by the regional patterns of barotropic deformation in the upper troposphere.

Although many previous studies have examined the factors regarding the variations of storm track activity, fundamental questions are still not fully understood. Particularly, Mak and Deng (2007) pointed out four unresolved features of the storm track activity: different intensities of the PST and AST activities, difference in the intraseasonal variability of the activity of the two storm tracks, natures of interannual/decadal variability of the storm track activities, and roles of moist processes on storm tracks dynamics. While many previous studies have focused on the midwinter minimum of the PST activity and its possible causes, comparison of the activity of the two storm tracks and their interaction with mean flow in subseasonal time scale have been studied little. In particular, it has not been clearly understood how barotropic and baroclinic energetics differently contributes to the initiation and enhancement of the activity of the two storm tracks. Since the background flow and transient eddy fluxes vary with time and region, the energy conversion between mean flow and eddy should change with time and region and play different roles on the activity of the two storm tracks in subseasonal variation. The main purpose of the present study is to understand mechanisms affecting intensities and subseasonal variations of the climatological PST and AST activities. Particular attention is paid to the different roles of barotropic and baroclinic energetics on the midwinter minimum of the PST activity and midwinter maximum of the AST activity.

The data and analysis methods used in the study are presented in Sect. 2. Section 3 describes the contrasting storm track–jet stream relationships between the North Pacific and North Atlantic that is one of the major issues in storm track dynamics. In Sects. 4 and 5, we discuss causes that may be responsible for the contrasting relationships from barotropic and baroclinic (Sect. 4) and moisture (Sect. 5) point of view. Section 6 summarizes our results.

2 Data and analysis methods

We used the National Centers for Environmental Prediction/Department of Energy (NCEP-DOE) AMIP-II Reanalysis data set (NCEP-2; Kanamitsu et al. 2002) for the daily horizontal winds and vertical motion, geopotential height, temperature, and precipitable water from 1979 to 2008. Since NCEP-2 does not provide specific humidity on pressure level, specific humidity is derived from relative humidity.

Previous studies have used several band-pass filtered quantities to represent the storm track intensities which include meridional velocity variance (Chang and Fu 2002; Orlanski 2005), northward eddy heat flux (Nakamura 1992;Chang and Guo 2007), EKE (Black and Dole 2000; Williams et al. 2007; Nie et al. 2008), and the root-mean-square (RMS) of the synoptic component of the geopotential height (Blackmon et al. 1977; Hurrell and van Loon 1997; Mak and Deng 2007). Chang (2009) examined several different band-pass filtered statistics, and suggested that band-pass filtered variances are useful indicators of the storm track activity. In this study, we tested aforementioned quantities for presenting the storm track activity and

chose the RMS of 2–8 day band-pass filtered meridional wind.

For better understanding the subseasonal variation of the activity of the two storm tracks, local energetics in terms of barotropic energy conversion (BTEC) and BCEC is investigated in the quasi-geostrophic framework based on Cai et al. (2007). The BTEC is produced by the inner product of deformation vector (D-vector) of the time mean flow and eddy vector (E-vector). The BCEC from mean available potential energy (MAPE) to eddy available potential energy (EAPE) is obtained from the product of horizontal eddy heat flux and time mean temperature gradient. In addition, the BCEC between EAPE and EKE can be expressed by upward eddy heat flux.

3 Subseasonal variation of the storm track activity

To begin with, the climatological subseasonal variation of the activity of the two storm tracks in the NH is compared in terms of their spatial-temporal structures along with the jet stream variations. The monthly mean storm track intensity is defined by the RMS of 2–8 day band-pass filtered meridional wind in each calendar month and its climatological monthly mean is obtained by averaging over the period of 1979–2008.

Figure 1 shows the climatological monthly mean storm track intensity and westerly jet at 300-hPa in the North Pacific and the North Atlantic from November to March. Two contrasting features between the activity of the two storm tracks are noteworthy. First, the PST activity tends to be weakened and its core shifts southward from fall (50°N) to midwinter (40°N) in spite of the strongest jet in January, whereas the AST activity remains steady in longitudinal and latitudinal position and peaks in midwinter, which has been noted in many previous studies (Nakamura 1992; Chang et al. 2002; Mak and Deng 2007 among others). Second, although jet intensity and thus baroclinicity are much weaker in the North Atlantic than in the North Pacific, the AST intensity is much stronger than the PST intensity during midwinter. We note also that the maximum PST activity locates in further downstream and north of the Pacific jet core. The AST activity center is located slightly downstream of the Atlantic jet core.

Longitudinal and latitudinal averages of the storm track intensity along the variability center show more distinct difference between the two storm tracks in seasonal evolution. Figure 2 exhibits time-latitude structure of the storm track activity and zonal wind at the three vertical levels. It is noted that the PST is shifted southward and weakened as the Pacific jet shifts southward and enhanced from October to January, while the AST tends to persist in locating around 50°N and intensify in midwinter with the maximum Atlantic jet at all three levels as pointed out by Nakamura (1992) and Nakamura et al. (2002). Nakamura and Sampe (2002) also showed the latitudinal displacement between the storm track axis and jet axis in the North Pacific. The contrasting storm track–jet relationship between the North Pacific and the North Atlantic remains an elusive issue. In the next sections, we discuss causes that may be responsible for the contrasting storm track–jet relationships by analyzing barotropic and baroclinic energetics.

4 Barotropic and baroclinic energetics

In this study, local perturbation kinetic energy (K_e) and the local perturbation potential energy (P_e) are focused because the energy of perturbation is important for the developing the storm track activity. Following Cai and Mak (1990) and Deng and Mak (2005), the time evolution of K_e and P_e can be expressed as follow.

$$\frac{\partial K_e}{\partial t} = -\mathbf{v}\cdot\nabla K_e - \nabla\cdot(\phi_a \mathrm{v} + \phi \mathrm{v}_d) - \frac{\partial \omega\phi}{\partial p} + \mathrm{E}\cdot\mathrm{D} - \mathrm{F}_{(3)}\mathrm{T}_{(3)} \tag{1}$$

$$\frac{\partial P_e}{\partial t} = -\mathbf{v}\cdot\nabla P_e + \mathrm{F}\cdot\mathrm{T} \tag{2}$$

where

$$\mathrm{E} = \left(\frac{1}{2}\left(\overline{v'^2} - \overline{u'^2}\right), -\overline{u'v'}\right),$$

$$\mathrm{D} = \left(\frac{\partial \overline{u}}{\partial x} - \frac{\partial \overline{v}}{\partial y}, \frac{\partial \overline{v}}{\partial x} + \frac{\partial \overline{u}}{\partial y}\right),$$

$$\mathrm{F} = \Re(u'\theta, v'\theta, -\omega'\theta),$$

$$\mathrm{T} = \left(\frac{\partial \Theta_0}{\partial p}\right)^{-1}\left(\frac{\partial \Theta}{\partial x}, \frac{\partial \Theta}{\partial y}, -\frac{\partial \Theta}{\partial p}\right),$$

$$\Re = \frac{\mathrm{R}}{\mathrm{p}_0}\left(\frac{\mathrm{p}_0}{\mathrm{p}}\right)^{\mathrm{C_v}/\mathrm{C_p}}$$

An overbar represents the climatological mean, p_0 is 1,000 hPa, and R is the gas constant for dry air. The u' and v' are transient zonal and meridional wind, respectively. And, ω' is transient vertical p-velocity. C_P (C_V) represents the specific heat of dry air at the constant pressure (volume) and Θ stands for potential temperature. The subscript "3" refers to the vertical component. The term $E \cdot D$ represents the BTEC and the term $F \cdot T$ which has two part, i.e. $F_h \cdot T_h$ and $-F_{(3)}T_{(3)}$, indicates the net generation of perturbation potential energy. The term $F_h \cdot T_h$ and $-F_{(3)}T_{(3)}$ represent conversion from MAPE to EAPE and conversion from EAPE to EKE, respectively. The subscript "h" means the horizontal component. The v_d is the irrotational part of the ageostrophic wind, and ϕ_a is the ageostrophic part of the geopotential. More details on local

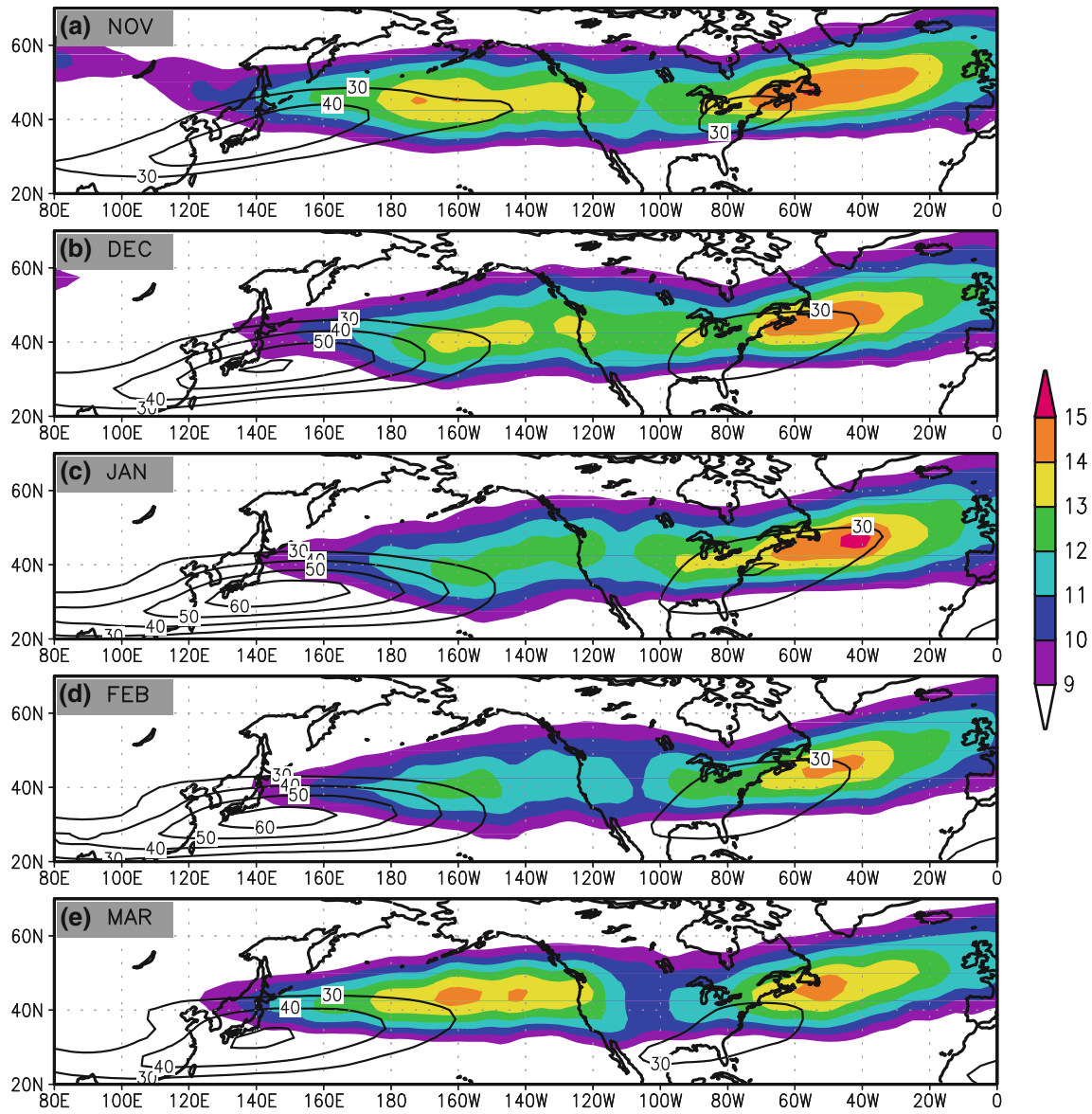

Fig. 1 Root-mean-square of the 2–8 day band-pass filtered 300-hPa meridional wind (m s^{-1}) (*shading*), 300-hPa zonal wind (m s^{-1}) (*contour*) in **a** November, **b** December, **c** January, **d** February, and **e** March averaged from 1979 to 2008. The contour level of zonal wind is 30, 40, 50, 60 m s^{-1}

energetics can be found in Cai and Mak (1990) and Deng and Mak (2005). The equation for the budget of the total local perturbation energy (TE) can be obtained from the sum of Eqs. 1 and 2.

$$\frac{\partial \mathrm{TE}}{\partial \mathrm{t}} = -\mathbf{v}\cdot\nabla \mathrm{TE} - \nabla\cdot(\phi_{\mathrm{a}}\mathrm{v} + \phi \mathrm{v}_{\mathrm{d}}) - \frac{\partial \omega\phi}{\partial \mathrm{p}} + \mathrm{E}\cdot\mathrm{D} + \mathrm{F}_{\mathrm{h}}\cdot\mathrm{T}_{\mathrm{h}}$$

Since advection of energy and convergence of energy flux only redistribute the perturbation energy, just BTEC and BCEC terms are considered and further analysis methods on BTEC and BCEC will be shown in next sections.

4.1 Eddy shape and orientation

The barotropic component of the background flow can exert an influence on the storm track structure (Branstator 1995). Using the linear barotropic model, Lee (2000) showed that the barotropic dynamics alone can produce some essential features of the observed storm track structure when the model flow is initialized with a realistic wave packet. Before the evaluation of BTEC, the local shape and horizontal orientation of eddies over the two storm tracks are first compared using E-vector based on Trenberth (1986). It differs from the E-vector of Hoskins et al. (1983) by a factor of 1/2 in

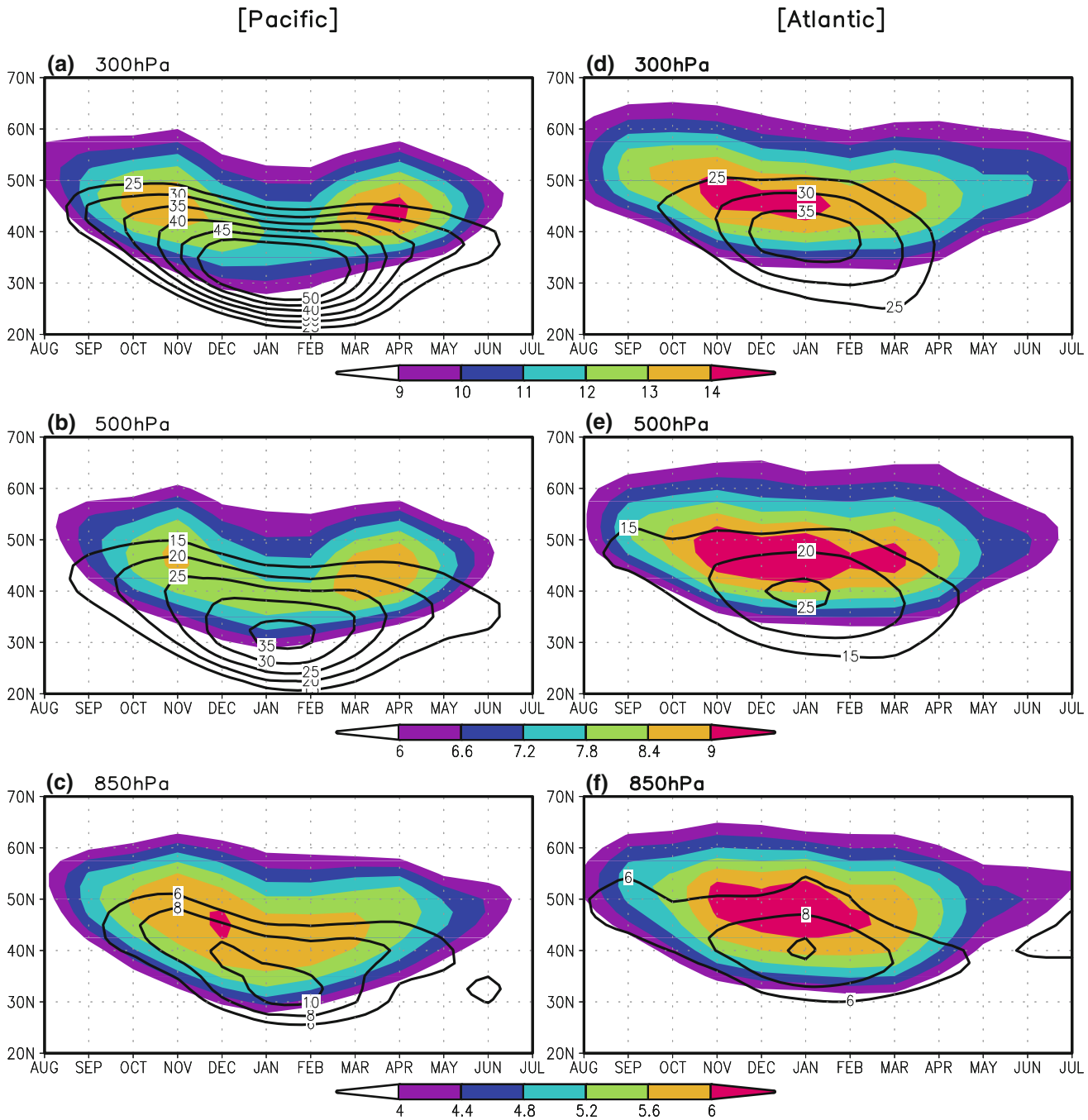

Fig. 2 Time-latitude cross section of storm track intensity (m s^{-1}) (*shading*) and zonal wind (m s^{-1}) (*contour*) over the **a–c** Pacific and **d–f** Atlantic at 300-hPa (*upper panels*), 500-hPa (*middle panels*) and 850-hPa (*lower panels*). To obtain longitudinal mean, storm track activity was averaged between 175°E–145°W (70°–30°W) and jet stream was averaged between 130°–170°E (90°–50°W) in the Pacific (Atlantic)

the x-component (Mak and Cai 1989). The x-component of E-vector is related to the degree of meridional elongation and the y-component is related to an axial tilt and westerly momentum transport by transient eddies.

Figure 3 shows subseasonal evolution of the E-vector for band-pass filtered transient eddies (2–8 days). Two prominent differences are seen between the PST and AST. First, the orientation of the E-vector is evidently different in the two storm track regions. Over the North Pacific E-vector points southward, implying that eddies tend to be less anisotropic and their axial tilt is relatively large. Over North America and the North Atlantic E-vector points eastward, implying that eddies are more meridionally elongated and their axial tilt is relatively small. The

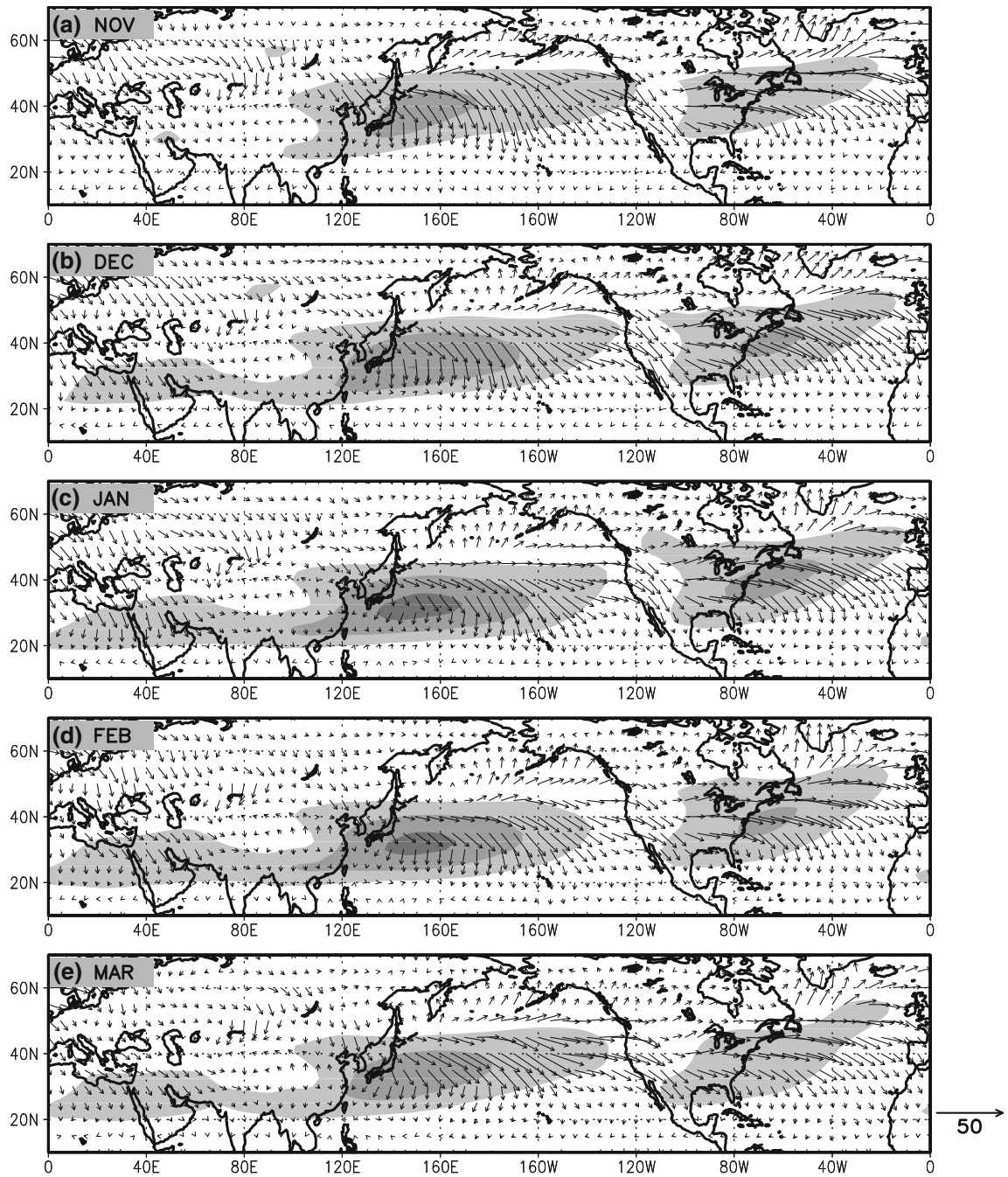

Fig. 3 The E-vector for band-pass filtered transient eddies (2–8 days) in **a** November, **b** December, **c** January, **d** February, and **e** March (1979–2008). The shadings indicate 500-hPa zonal wind and shading level is 15, 25, 35 m s^{-1}

reduced anisotropy and large axial tilt of eddies over the Pacific is evident only along the storm track and its south, while the axial tilting comparable to its Atlantic counterpart is evident only on the poleward flank of the Pacific storm track. The E-vector is much larger over the jet entrance region in the Atlantic than the Pacific. Difference of E-vector between two storm track regions plays a critical role on BTEC which will be shown later. Second, the E-vector gets weaken particularly over the jet entrance (20°–40°N, 120°–160°E) and downstream region (30°–50°N, 140°–120°W) from fall to midwinter in the Pacific regardless of strong jet intensity, whereas over the entire AST region this is not the case. The weakening of the E-vector in the Pacific is due in part to the weakening of transient eddies manifested as the midwinter minimum of the storm track activity.

4.2 Barotropic energy conversion

The BTEC can be expressed by the inner product of D-vector of the basic flow and E-vector of the transient parts (Cai et al. 2007).

$$\mathrm{BTEC} = \frac{p_0}{g}\left\{\frac{1}{2}\left(\overline{v'^2} - \overline{u'^2}\right)\left(\frac{\partial \overline{u}}{\partial x} - \frac{\partial \overline{v}}{\partial y}\right) + \left(-\overline{u'v'}\right)\left(\frac{\partial \overline{v}}{\partial x} + \frac{\partial \overline{u}}{\partial y}\right)\right\}$$

where g is the acceleration of gravity. Figure 4 exhibits the vertical distribution of kinetic energy conversion from the time mean flow to transient eddies along 30°–50°N in November and January. Positive (negative) values indicate that eddies gain (lose) energy from (to) the mean flow. The corresponding storm track activity is superimposed. The figure indicates three important points. First, BTEC plays an important role on the initial growth of eddies along the two storm tracks. Eddies gain kinetic energy at the entrance region of storm tracks while barotropic damping is dominant along the center and downstream regions of two storm tracks. Lee (2000) also indicated that positive BTEC is found in the upstream of the two storm tracks and the geographical location of positive BTEC contributes to the eddy growth in the storm tracks. Second, BTEC is mainly confined in the upper troposphere centered at 300-hPa. Third, BTEC over the Atlantic is much larger than that over the Pacific in January, while those are comparable to each other in November. The weakening of BTEC over the Pacific in January in spite of the strongest jet stream suggests that the eddy properties should play more crucial role on determining eddy-mean flow interaction than intensity of background deformation.

To better understand the relative contribution of the background deformation and eddy properties on BTEC between the two storm tracks, the energy conversion in January is decomposed into the stretching and shearing deformation terms. The stretching (shearing) deformation term is defined as the product of x (y)-component of E-vector and that of D-vector. Figure 5a and d show very clear difference of barotropic energetics between the two storm tracks. The shearing (stretching) deformation term is more dominant in the PST (AST) in January. Because of significant value of E-vector's x-component over North America and the North Atlantic (Fig. 5b), contribution of stretching deformation is much larger over the regions although stretching of basic flow is comparable between the two storm track regions (Fig. 5c). On the other hand, much stronger horizontal wind shear in East Asia and the North Pacific (Fig. 5f) is responsible for larger contribution of BTEC in the regions when eddies show comparable axial tilting and then horizontal momentum flux in the two storm track regions (Fig. 5e). However, it is of importance to note that the strongest background shearing deformation

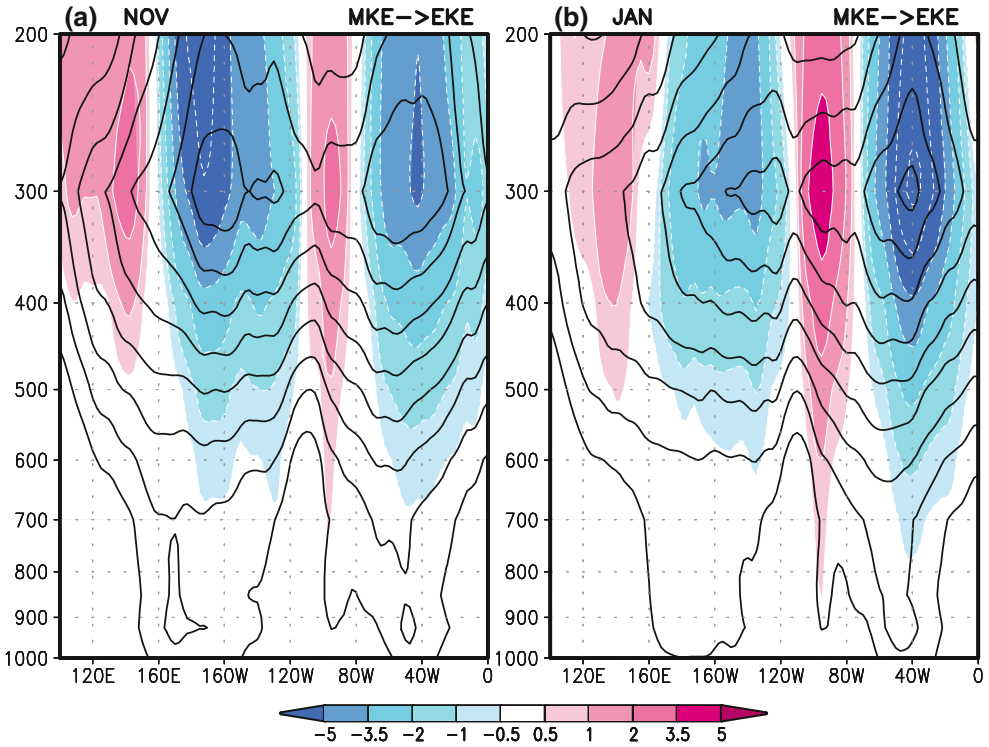

Fig. 4 Vertical-longitude cross section of kinetic energy conversion from the mean flow to eddies (W m^{-2}) along 30°–50°N in **a** November and **b** January. Contours in **a** and **b** indicate the storm track activity along 37.5°–57.5°N (contour level: 5, 6, …, 12, 13 m s^{-1})

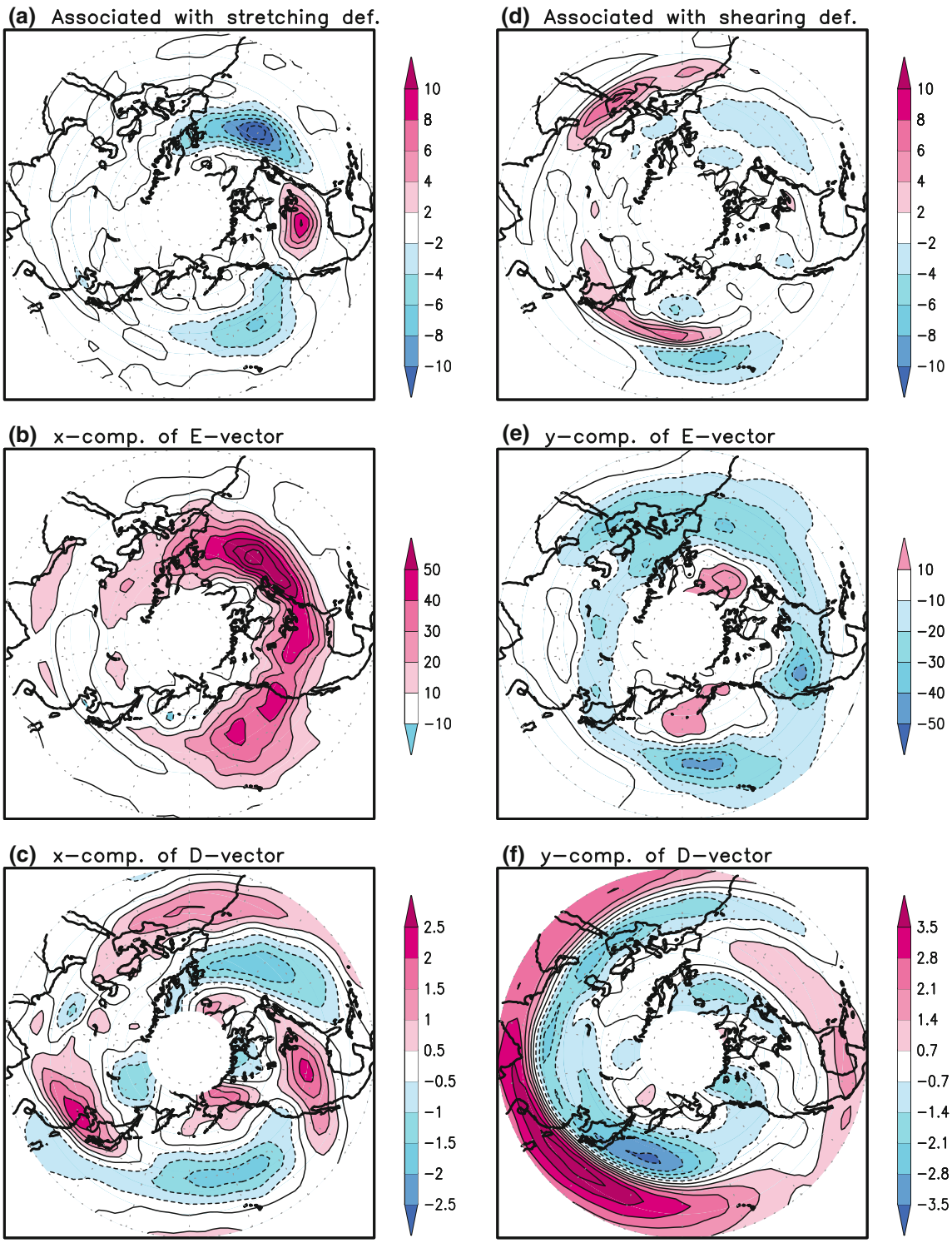

Fig. 5 Kinetic energy conversion at 300-hPa in January related to the **a** stretching deformation and **d** shearing deformation. **b** x-component of E-vector (m^2s^{-2}) and **c** x-component of D-vector ($\times 10^{-5}$ s^{-1}). **e** y-component of E-vector (m^2s^{-2}) and **f** y-component of D-vector ($\times 10^{-5}$ s^{-1})

(Fig. 5f) in January less contributes to eddy development than weaker counterpart in November because eddy's axial tilting is smaller in January than in November over the entrance region of the PST (not shown).

4.3 Baroclinic energy conversion

Previous studies have shown that baroclinic instability is the primary mechanism generating transient eddies that

compose the storm tracks (Blackmon et al. 1977; Lindzen and Farrell 1980; Pierrehumbert and Swanson 1995; Frisius et al. 1998; Chang et al. 2002; Cai et al. 2007). We further compare the local baroclinic energetics between the two storm tracks.

Figure 6 shows vertical wind shear and the maximum Eady growth rate $\left(\sigma = 0.31\left|\frac{f}{N}\frac{\partial U}{\partial z}\right|\right)$ (Lindzen and Farrell 1980) as indicator of baroclinicity in November and January, respectively. It is obvious that baroclinicity is the largest in January in both storm track regions and it is stronger in the North Pacific than in the North Atlantic where the upper-level jet and the vertical wind shear are larger. However, there are discrepancies in the core location of jet stream and that of baroclinicity, particularly over the Pacific. That is because the combined effect of Coriolis effect, which decreases with latitude, and the static stability, which decreases toward ocean, positions the maximum baroclinicity zone north-eastward from the maximum location of jet stream (Fig. 6d).

More specific baroclinic energy conversion is investigated in terms of the BCEC from MAPE to EAPE and from EAPE to EKE based on Cai et al. (2007). The BCEC from MAPE to EAPE is related to horizontal eddy heat flux and thermal gradient and is defined as,

$$\text{BCEC I} = -C_2\left(\overline{u'T'}\frac{\partial\overline{T}}{\partial x} + \overline{v'T'}\frac{\partial\overline{T}}{\partial y}\right),$$

$$C_2 = C_1\left(\frac{p_0}{p}\right)^{R/C_P}\Big/\left(-\frac{d\Theta}{dp}\right), \quad C_1 = \left(\frac{p_0}{p}\right)^{C_V/C_P}\frac{R}{g},$$

The BCEC from EAPE to EKE is defined as,

$$\text{BCEC II} = -C_1\left(\overline{\omega'T'}\right),$$

where T' is temperature perturbation.

The comparison of BCEC from MAPE to EAPE over the two storm tracks in November and January at 500-hPa is shown in Fig. 7a and c. In general, the maximum BCEC from MAPE to EAPE occurs at upstream of the two storm track cores. However, the distance between the cores of storm track and energy conversion is much larger in the North Pacific than in the North Atlantic like the storm track–jet relation. Moreover, the core region of maximum energy conversion in the North Pacific moves southward from November to January. It is noted that the BCEC from MAPE to EAPE increases during midwinter in the North Atlantic, while that in the North Pacific shows insignificant change.

BCEC from EAPE to EKE is presented in Fig. 7b, d. Similar to the BCEC from MAPE to EAPE (Fig. 7a, c), converting potential energy into kinetic energy of perturbations in the North Atlantic increases from November to January. By analysis of the eddy correlation statistics, Nakamura et al. (2002) showed that higher correlation between v' and T' (ω' and T') indicates more efficient BCEC from MAPE to EAPE (from EAPE to EKE). We also examine the correlation between ω' and T' in November and January. The correlation decreased from November to January in the North Pacific whereas it slightly increased in the North Atlantic (not shown). This implies that BCEC from EAPE to EKE becomes less efficient due to eddy structure changing from its optimal state as suggested in Nakamura et al. (2002).

Difference of BCEC between November and January is examined using vertical-longitude cross section as shown in Fig. 8. The vertical distribution of BCEC is obtained by latitudinal average over the maximum conversion region, namely (37.5°–57.5°N). The BCEC from MAPE to EAPE shows the maximum at the upper level in the Pacific, while

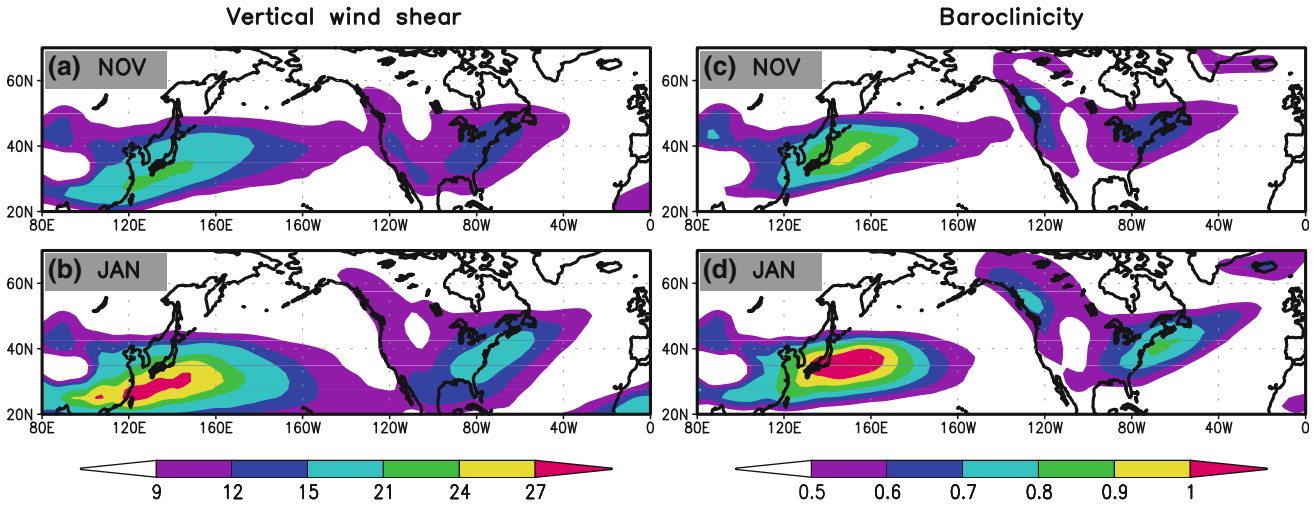

Fig. 6 Vertical shear of zonal wind between 850- and 500-hPa (*left panels*) and the Eady growth rate (day^{-1}) between 850- and 500-hPa (*right panels*) in **a**, **c** November and **b**, **d** January

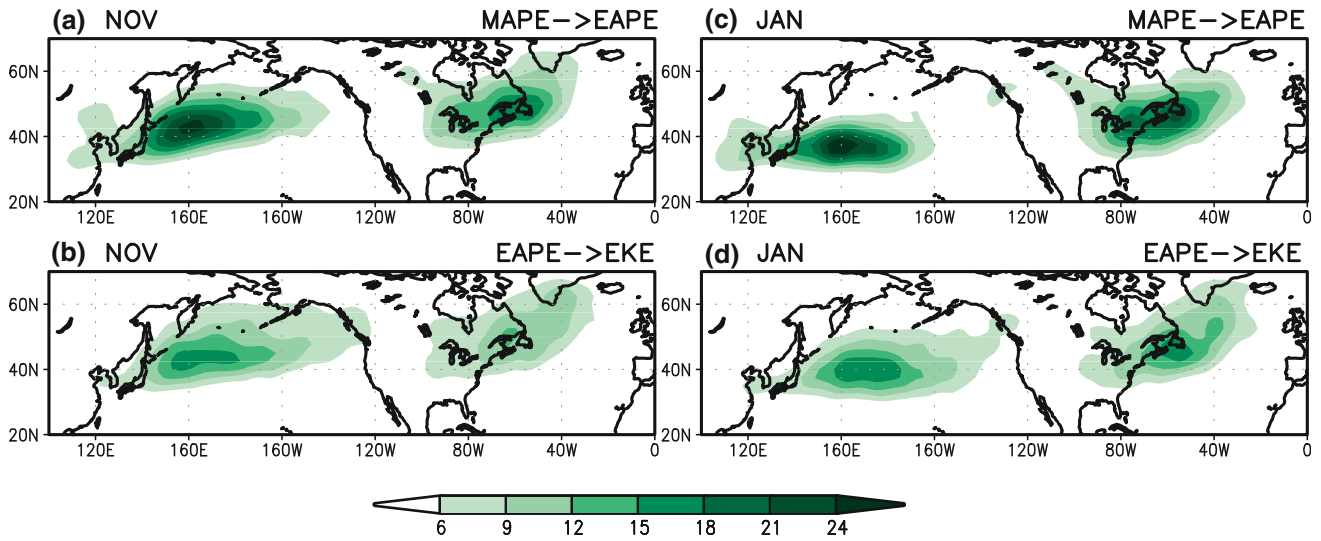

Fig. 7 Energy conversion from mean available potential energy to eddy available potential energy (W m^{-2}) (*upper panels*) and from eddy available potential energy to eddy kinetic energy (W m^{-2}) (*lower panels*) at 500-hPa in November (*left panels*) and January (*right panels*)

that is large at the low-level in the Atlantic. It is shown that the BCEC from EAPE to EKE has maximum at the mid-level. From November to January, baroclinic energy conversion in the Pacific decreases, particularly at upstream of the PST. In the Atlantic, however, baroclinic energy conversion significantly increases along the core of AST as well as in its upstream. Particularly, the enhanced BCEC from MAPE to EAPE at the low-level and from EAPE to EKE at the mid-level is very remarkable. The correlation between high-frequency fluctuations in temperature and meridional velocity at 850-hPa is also examined. Compared with November, the correlation greatly increased in January in the North Atlantic (not shown) and this means more efficient in converting the MAPE to EAPE.

Previously, we showed the evident increase of BCEC from MAPE to EAPE over the North Atlantic in January, particularly at low-level (Fig. 8c). In order to reveal which component plays major role in increasing this energy conversion during midwinter in the North Atlantic, BCEC from MAPE to EAPE at 850-hPa is decomposed. We just show meridional component of the BCEC from MAPE to EAPE in Fig. 9 since it is much larger than zonal component. The $\overline{v'T'}$ term is one of the primary flux associated with baroclinic instability and downgradient heat fluxes generate EAPE (Trenberth 1991). Poleward eddy heat flux is dominant in both the North Pacific and North Atlantic, and that increases over the North Atlantic in January. However, in the North Pacific, poleward eddy heat flux slightly decreased and moved southward in January. From November to January, the increased meridional temperature gradient is found along east coast of Eurasia and North America continent, and the maximum meridional temperature gradient in the North Pacific shifts southwestward. It is noted that the coincidence of core regions for meridional eddy heat flux and for meridional temperature gradient in the North Atlantic plays an important role in determining the magnitude of meridional component of BCEC from MAPE to EAPE (PEY). In the North Pacific, in spite of increase in meridional temperature gradient, magnitude of PEY in January is similar to that in November due to the longitudinal discrepancy of maximum $\overline{v'T'}$ and $\partial\overline{T}/\partial y$ regions.

5 Moisture effect

The argument presented in Sect. 4 is based on dry barotropic and baroclinic dynamics. However, the northeastward moving Kuroshio Current in the western North Pacific and Gulf Stream over the Atlantic can provide additional heat and moisture into the storm track regions, and influence the local baroclinic growth. Several recent studies showed that the heat supply from warm western boundary currents such as Kuroshio and Gulf Stream plays an important role in maintaining baroclinicity, and consequently helps the development of storm track activity (Nonaka et al. 2009; Taguchi et al. 2009; Sampe et al. 2010). Most explosive cyclone genesis cases in the storm track regions depend on condensational latent heat release in the baroclinic eddies (Sanders and Gyakum 1980). Based on the comparison between dry and moist development of baroclinic waves under the same zonal mean flow, Hayashi and Golder (1981) showed that eddy growth in the presence of latent heat release is enhanced not only by the eddy energy

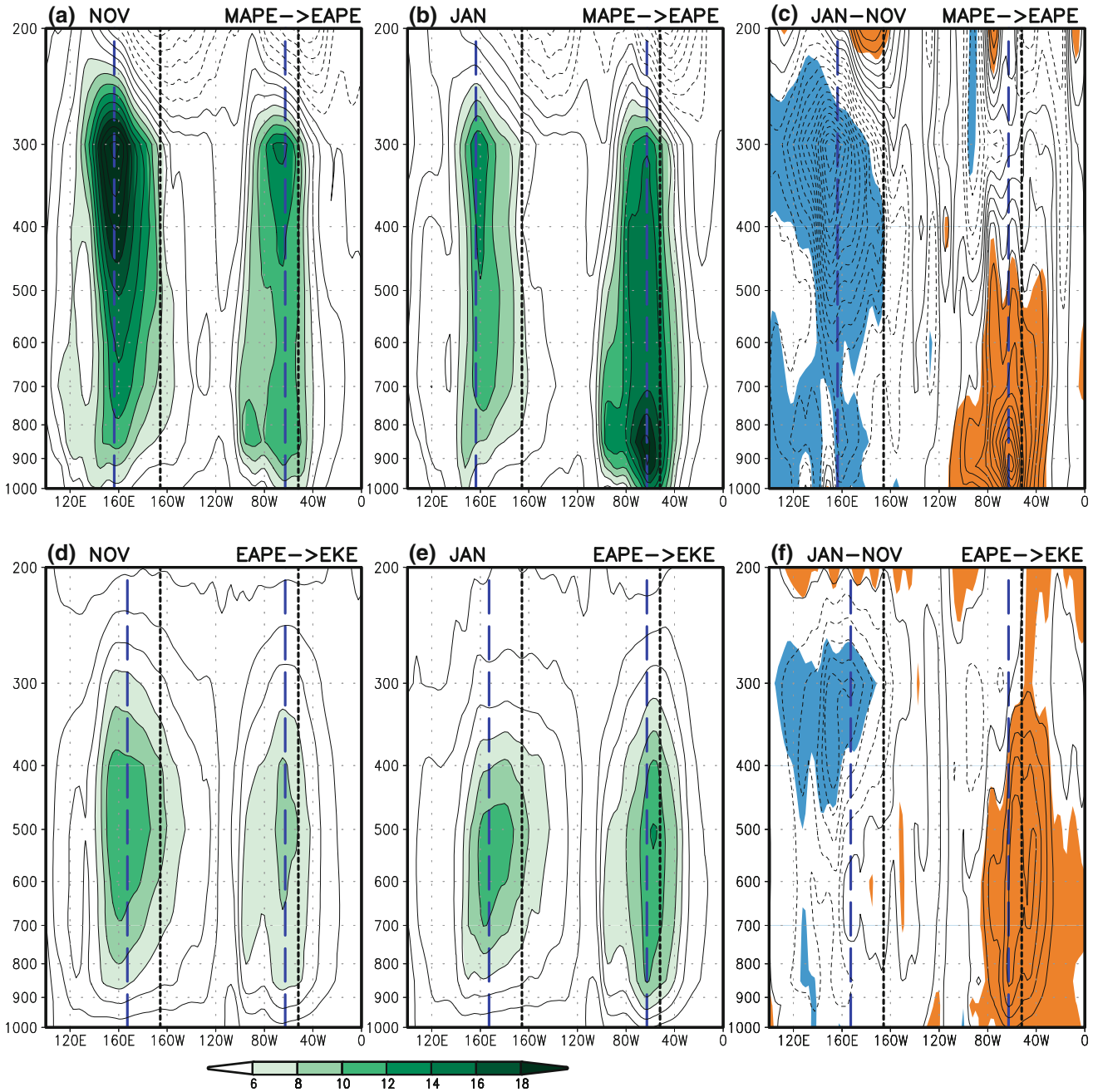

Fig. 8 Vertical-longitude cross sections of baroclinic energy conversion along 37.5°–57.5°N in **a**, **d** November, **b**, **e** January, and **c**, **f** its difference between 2 months. *Upper* (*lower*) *panels* indicate energy conversion from mean available potential energy to eddy available potential energy (from eddy available potential energy to eddy kinetic energy). *Shadings* in **c**, **f** represent the values significant at the 95% confidence level. The *thick dotted* and *dashed lines* indicate the axis of maximum storm track activity and baroclinic energy conversion, respectively

generated by the latent heat release but also by the fact that baroclinic energy conversion is strongly enhanced in the presence of moisture.

Using an extended moist Eady model, Wang and Barcilon (1986) have shown that the growth rate of the moist baroclinic instability, besides being dependent of vertical shear and Burger number, critically depends on the mean specific humidity in the boundary layer, which measures the latent heating intensity and the moist static energy stored in the mean flow. Both the APE, measured by the vertical shear, and the available moist energy, measured by the mean specific humidity and the depth of the moist convergent layer are important energy sources for the moist baroclinic unstable mode. In the particular

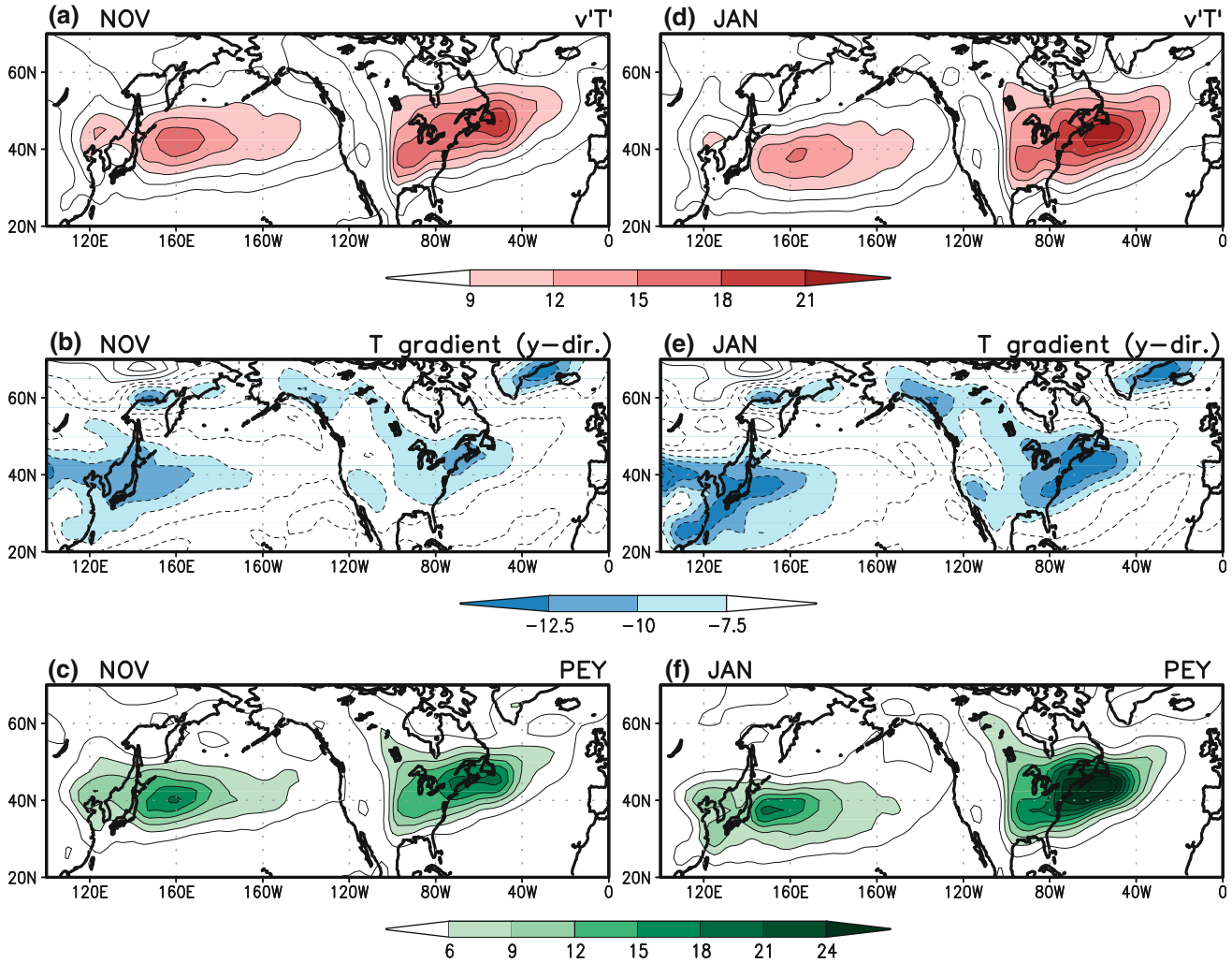

Fig. 9 Distribution of **a**, **d** meridional eddy heat flux ($\overline{v'T'}$) (km s^{-1}), **b**, **e** meridional temperature gradient ($\partial\overline{T}/\partial y$) ($\times 10^{-6}$ km^{-1}), and **c**, **f** $-C_2\left(\overline{v'T'}\frac{\partial\overline{T}}{\partial Y}\right)$ (PEY) (W m^{-2}) at 850-hPa in November (*left panels*) and January (*right panels*)

condition where the low-level static stability is reduced, dry baroclinic eddy growth itself could be enhanced, as suggested by the expression of Eady growth rate. This is through augmenting vertical motion, which can also enhance latent heat release.

In order to find out the role of moisture in upstream region of the storm tracks, characteristics of precipitable water is examined. Difference of precipitable water between January and November and subseasonal variation with storm track activity are presented in Fig. 10. The great decrease of precipitable water in January is evident in the North Pacific, particularly southeast of Japan, compared to in the North Atlantic. In subseasonal variation, the magnitude of precipitable water in upstream of the storm tracks is comparable in fall and spring over the Pacific and Atlantic. However, in midwinter, precipitable water in the Atlantic is relatively larger than that in the Pacific, particularly along the axis of energy conversion from MAPE to EAPE. This relatively large amount of precipitable water in midwinter over the Atlantic can induce considerable latent heat release, consequently be an extra source for the moist synoptic scale wave growth.

The meridional moisture flux is important because it has an influence on local precipitation and evaporation and represents a latent heat flux (O'Gorman and Schneider 2008). Raphael (1997) examined the relationship between the meridional eddy sensible heat ($\overline{v'T'}$) and latent heat fluxes ($\overline{v'q'}$) and showed that these fluxes are most strongly correlated in the storm tracks. Figure 11 illustrates the characteristics of meridional eddy moisture flux in November and January by means of the longitude-pressure cross section. It is noted that meridional eddy moisture flux in November shows the maximum along the axis of BCEC from MAPE to EAPE in both the Pacific and Atlantic. The

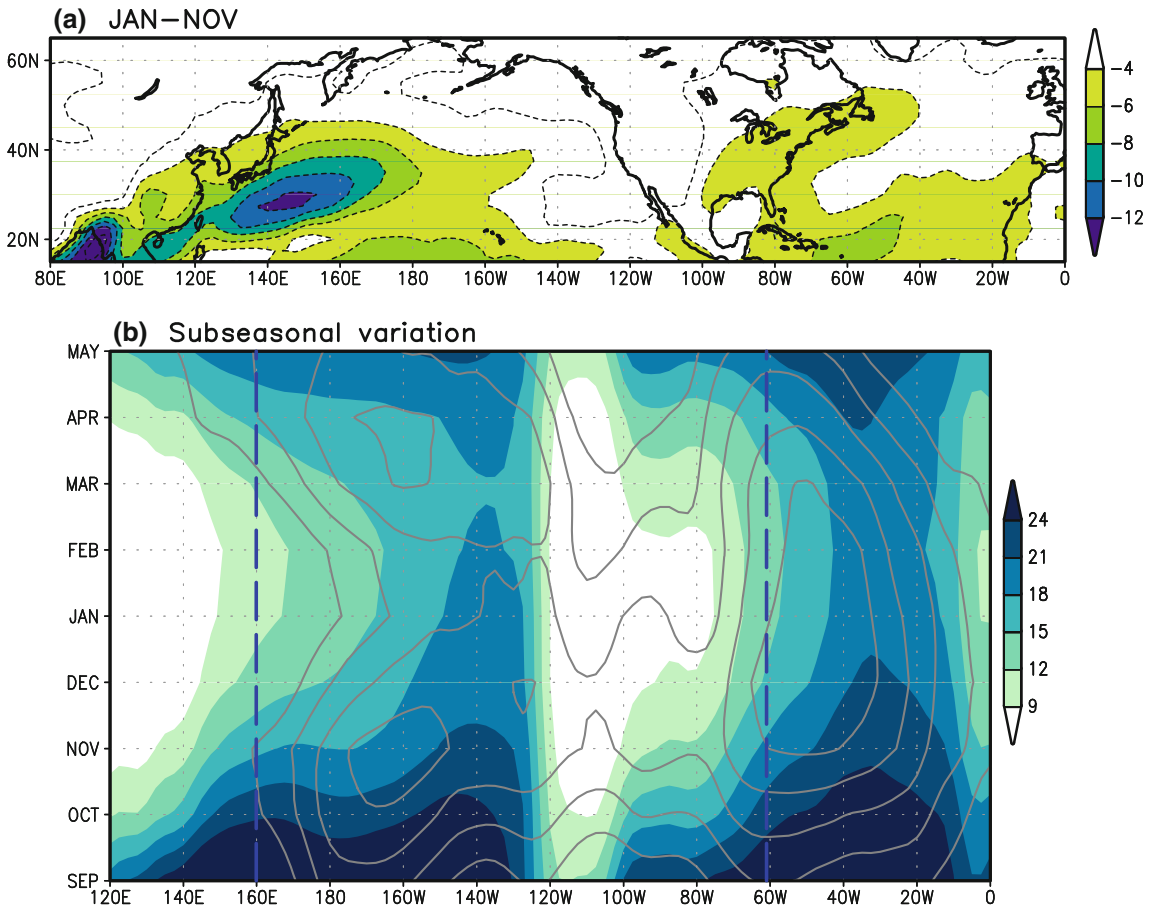

Fig. 10 **a** Difference of precipitable water (kg m^{-2}) between January and November and **b** time-longitude cross section of precipitable water (kg m^{-2}) (*shading*) and storm track intensity (m s^{-1}) (*contour*). Contour interval is 0.6 m s^{-1} and storm track intensity less than 10 m s^{-1} is omitted. For the precipitable water and storm track intensity, the latitudinal band of (35°–50°N) and (37.5°–57.5°N) is averaged, respectively. The *dashed lines* indicate the axis of maximum energy conversion from MAPE to EAPE

meridional eddy moisture flux significantly decreases over the Pacific in January, whereas that shows slight increase in the AST. In midwinter, precipitable water (Fig. 10) and meridional eddy moisture flux (Fig. 11) are significantly larger over the Atlantic than the Pacific, which indicates that larger latent heat release plays a certain role on the stronger storm track activities and eddy-mean interaction over the Atlantic.

6 Summary and discussion

The remarkable differences of barotropic and baroclinic energetics related to the contrasting storm track–jet relationship over the North Pacific and North Atlantic are investigated using NCEP-2 reanalysis data for the period of 1979–2008. Previous studies have shown that from fall to midwinter the PST activity weakens following the southward shift of the Pacific jet, but the AST activity remains steady in position and peaks in midwinter regardless of the slight southward shift of the Atlantic jet. We have confirmed the previous findings that the AST intensity is stronger than the PST intensity during midwinter although the winter jet stream is much stronger over the North Pacific than the North Atlantic.

Eddy properties including eddy shapes and its axial tilt are noticeably different over the North Pacific and North Atlantic. Over the North Pacific, the eddy shapes are near isotropic, but over the North Atlantic, eddies are more meridionally elongated. Because of strong meridional elongation of eddies, contribution of stretching deformation term plays major role in the initiation of the AST although stretching of basic flow is comparable between the two storm track regions. On the other hand, the shearing deformation term stemming from much stronger horizontal wind shear in East Asia and the North Pacific is responsible for the genesis of the PST.

Analysis of BCEC suggests that transient eddies should grow more efficiently over the North Atlantic than the North Pacific because core regions of poleward and upward

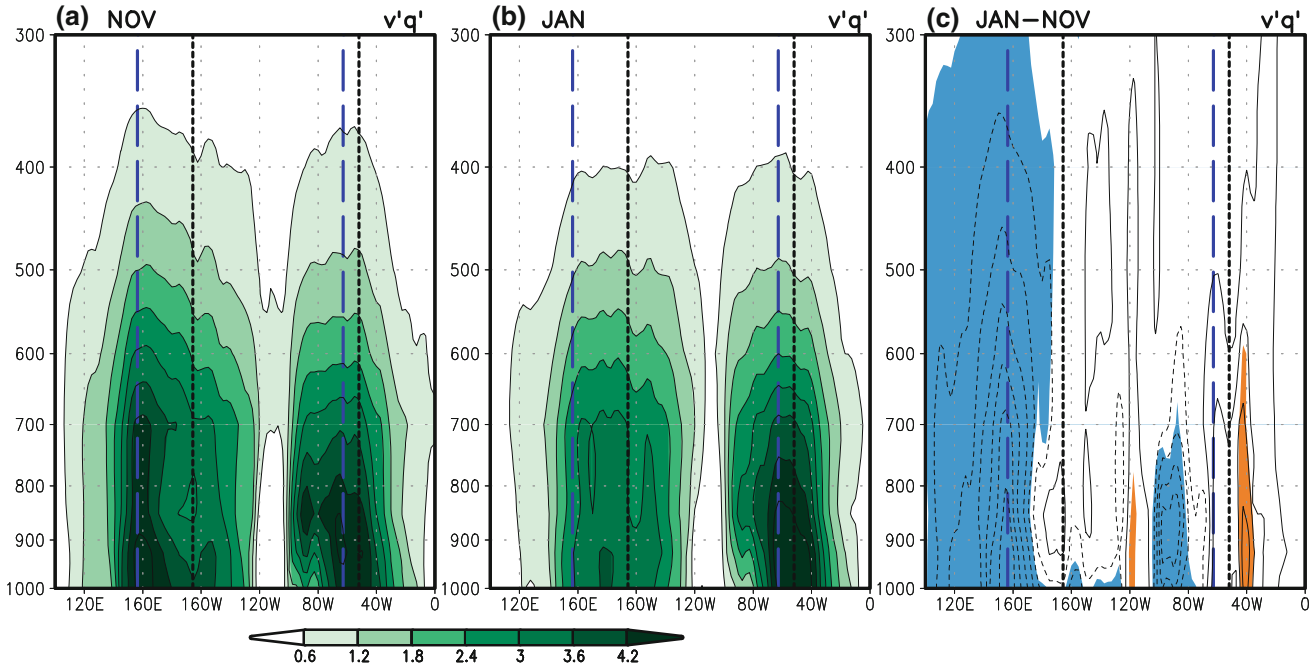

Fig. 11 Vertical-longitude cross section of meridional eddy moisture flux (m s^{-1} gKg^{-1}) along 35°–50°N in **a** November, **b** January, and **c** its difference. *Shadings* in **c** represent the values significant at the 95% confidence level. The *thick dotted* and *dashed lines* indicate the axis of maximum storm track activity and baroclinic energy conversion, respectively

eddy heat fluxes are coincident with that of meridional temperature gradient. And, the structure of eddies becomes optimum for BCEC in midwinter as pointed out by Nakamura et al. (2002). In the slight upstream of the AST, poleward and upward eddy heat flux is enhanced concurrent with the increase of background baroclinicity which in turn amplifies the BCEC from mean flow to eddy. Furthermore, relatively large amount of precipitable water which can contribute to latent heat release and greater eddy moisture flux along the BCEC axis bring benefit to the strong AST activity in midwinter. On the other hand, the midwinter minimum of the PST intensity is mainly attributable to southward shift of the Pacific jet stream which leads to discrepancy between core regions of poleward and upward eddy heat flux and that of meridional thermal gradient, and consequently the decrease of BCEC over far upstream of the PST. Weakening of eddy-mean flow interaction due to eddy shape and reduction of moist effect are also responsible for the weakening of storm track activities in midwinter.

In the present study, we focused on the climatological features of the storm track–jet relationship in the North Pacific and North Atlantic in subseasonal time scale by analyzing transient eddy properties and barotropic and baroclinic energetics. Further studies in interannual and interdecadal time scales may be helpful for better understanding of the relationship. In addition, more detailed analysis is needed to quantify the amount of contribution from moisture effect on the difference of storm track activities.

Acknowledgments This work was supported by a grant from the Korean Ministry of Environment as "Eco-technopia 21 project" and the second stage of the Brain Korea 21 Project. J.-Y. Lee and Wang acknowledge support from Korean Meteorological Administration Research and Development Program under grant RACS 2010-2017 and from IPRC, which is in part supported by JAMSTEC, NOAA, and NASA. This is SOEST publication number 8089 and IPRC publication number 750.

References

Black RX, Dole RM (2000) Storm tracks and barotropic deformation in climate models. J Clim 13:2712–2728

Blackmon ML, Wallace JM, Lau NC, Mullen SL (1977) An observational study of the northern hemisphere wintertime circulation. J Atmos Sci 34:1040–1053

Branstator G (1995) Organization of storm track anomalies by recurring low-frequency circulation anomalies. J Atmos Sci 15:207–226

Cai M, Mak M (1990) On the basic dynamics of regional cyclogenesis. J Atmos Sci 47:1417–1442

Cai M, Yang S, Van den Dool HM, Kousky VE (2007) Dynamical implications of the orientation of atmospheric eddies: a local energetics perspective. Tellus 59A:127–140

Chang EKM (2001) GCM and observational diagnoses of the seasonal and interannual variations of the Pacific storm track during the cool season. J Clim 58:1784–1800

Chang EKM (2009) Are band-pass variance statistics useful measures of storm track activity? Re-examining storm track variability

associated with the NAO using multiple storm track measures. Clim Dyn 33:277–296
Chang EMK, Fu Y (2002) Interdecadal variations in northern hemisphere winter storm track intensity. J Clim 15:642–658
Chang EMK, Guo Y (2007) Dynamics of the stationary anomalies associated with the interannual variability of the midwinter Pacific storm track-the roles of tropical heating and remote eddy forcing. J Atmos Sci 64:2442–2461
Chang EMK, Lee S, Swanson KL (2002) Storm track dynamics. J Clim 15:2163–2183
Deng Y, Mak M (2005) An idealized model study relevant to the dynamics of the midwinter minimum of the Pacific storm track. J Atmos Sci 62:1209–1225
Deng Y, Mak M (2006) Nature of the differences in the intraseasonal variability of the Pacific and Atlantic storm tracks: a diagnostic study. J Atmos Sci 63:2602–2615
Frisius T, Lunkeit F, Fraedric K, James IN (1998) Storm-track organization and variability in a simplified atmospheric global circulation model. Q J R Meteorol Soc 124:1019–1043
Greeves CZ, Pope VD, Stratton RA, Martin GM (2007) Representation of northern hemisphere winter storm tracks in climate models. Clim Dyn 28:683–702
Hayashi Y, Golder DG (1981) The effects of condensational heating on midlatitude transient waves in their mature stage: control experiments with a GFDL GCM. J Atmos Sci 38:2532–2539
Hoskins BJ, James IN, White GH (1983) The shape, propagation, and mean-flow interaction of large-scale weather systems. J Atmos Sci 40:1595–1612
Hurrell JW, van Loon H (1997) Decadal variations in climate associated with the North Atlantic oscillation. Clim Change 36:301–326
Kanamitsu M, Ebisuzaki W, Woollen J, Yang SK, Hnilo JJ, Fiorino M, Potter GL (2002) NCEP-DOE AMIP-II reanalysis (R-2). Bull Am Meteorol Soc 83:1631–1643
Lee S (2000) Barotropic effects on atmospheric storm tracks. J Atmos Sci 57:1420–1435
Lindzen RS, Farrell BJ (1980) A simple approximate result for the maximum growth rate of baroclinic instabilities. J Atmos Sci 37:1648–1654
Mak M, Cai M (1989) Local barotropic instability. J Atmos Sci 46:3289–3311
Mak M, Deng Y (2007) Diagnostic and dynamical analyses of two outstanding aspects of storm tracks. Dyn Atmos Oceans 43:80–99
Nakamura H (1992) Midwinter suppression of baroclinic wave activity in the Pacific. J Atmos Sci 49:1629–1642
Nakamura H, Sampe T (2002) Trapping of synoptic scale disturbances into the North Pacific subtropical jet core in midwinter. Geophys Res Lett 29:1761. doi:10.1029/2002GL015535
Nakamura H, Izumi T, Sampe T (2002) Interannual and decadal modulations recently observed in the Pacific storm track activity and East Asian winter monsoon. J Clim 15:1855–1874
Nie J, Wang P, Yang W, Tan B (2008) Northern hemisphere storm tracks in strong AO anomaly winters. Atmos Sci Lett 9:153–159
Nonaka M, Nakamura H, Taguchi B, Komori N, Yoshida-Kuwano A, Takaya K (2009) Air-sea heat exchanges characteristic to a prominent midlatitude oceanic front in the South Indian Ocean as simulated in a high-resolution coupled GCM. J Clim 22:6515–6535
O'Gorman PA, Schneider T (2008) The hydrological cycle over a wide range of climates simulated with an idealized GCM. J Clim 21:3815–3832
Orlanski I (2005) A new look at the Pacific storm track variability: sensitivity to tropical SSTs and to upstream seeding. J Atmos Sci 62:1367–1390
Pierrehumbert RT, Swanson KL (1995) Baroclinic instability. Annu Rev Fluid Mech 27:419–467
Raphael MN (1997) The relationship between the transient, meridional eddy sensible and latent heat flux. J Geophys Res 102:13487–13494
Sampe T, Nakamura H, Goto A, Ohfuchi W (2010) Significance of a midlatitude SST frontal zone in the formation of a storm track and an eddy-driven westerly jet. J Clim 23:1793–1814
Sanders F, Gyakum JR (1980) Synoptic-dynamic climatology of the bomb. Mon Wea Rev 108:1589–1606
Taguchi B, Nakamura H, Nonaka M, Xie SP (2009) Influences of the Kuroshio/Oyashio extensions on air–sea heat exchanges and storm-track activity as revealed in regional atmospheric model simulations for the 2003/04 cold season. J Clim 22:6536–6560
Trenberth KE (1986) An assessment of the impact of transient eddies on the zonal flow during a blocking episode using localized Eliassen-Palm flux diagnostics. J Atmos Sci 43:2070–2087
Trenberth KE (1991) Storm tracks in the Southern Hemisphere. J Atmos Sci 48:2159–2178
Wang B, Barcilon A (1986) Moist stability of a baroclinic zonal flow with conditionally unstable stratification. J Atmos Sci 43:705–719
Williams RG, Wilson C, Hughes CW (2007) Ocean and atmosphere storm tracks: the role of eddy vorticity forcing. J Phys Oceanogr 37:2267–2289